

Multimodality analysis confers a prognostic benefit of a T-cell infiltrated tumor microenvironment and peripheral immune status in patients with melanoma

Georgia M Beasley ^{1,2}, Michael C Brown,³ Norma E Farrow,¹ Karenia Landa,¹ Rami N Al-Rohil,⁴ Maria Angelica Selim,⁴ Aaron D Therien,¹ Sin-Ho Jung,⁵ Junheng Gao,⁵ David Boczkowski,¹ Eda K Holl,¹ April K S Salama,² Darell D Bigner,^{2,3,4} Matthias Gromeier,^{2,3,6} Smita K Nair^{1,3,4}

To cite: Beasley GM, Brown MC, Farrow NE, *et al.* Multimodality analysis confers a prognostic benefit of a T-cell infiltrated tumor microenvironment and peripheral immune status in patients with melanoma. *Journal for ImmunoTherapy of Cancer* 2022;**10**:e005052. doi:10.1136/jitc-2022-005052

► Additional supplemental material is published online only. To view, please visit the journal online (<http://dx.doi.org/10.1136/jitc-2022-005052>).

GMB and MCB are joint first authors.

Accepted 05 September 2022



© Author(s) (or their employer(s)) 2022. Re-use permitted under CC BY-NC. No commercial re-use. See rights and permissions. Published by BMJ.

For numbered affiliations see end of article.

Correspondence to

Dr Georgia M Beasley;
georgia.beasley@duke.edu

Dr Smita K Nair;
smita.nair@duke.edu

ABSTRACT

Background We previously reported results from a phase 1 study testing intratumoral recombinant poliovirus, lerapolturev, in 12 melanoma patients. All 12 patients received anti-PD-1 systemic therapy before lerapolturev, and 11 of these 12 patients also received anti-PD-1 after lerapolturev. In preclinical models lerapolturev induces intratumoral innate inflammation that engages antitumor T cells. In the current study, prelerapolturev and postlerapolturev tumor biopsies and blood were evaluated for biomarkers of response.

Methods The following analyses were performed on tumor tissue (n=11): (1) flow cytometric assessment of immune cell density, (2) NanoString Digital Spatial profiling of protein and the transcriptome, and (3) bulk RNA sequencing. Immune cell phenotypes and responsiveness to in vitro stimulation, including in vitro lerapolturev challenge, were measured in peripheral blood (n=12).

Results Three patients who received anti-PD-1 therapy within 30 days of lerapolturev have a current median progression-free survival (PFS) of 2.3 years and had higher CD8+T cell infiltrates in prelerapolturev tumor biopsies relative to that of 7 patients with median PFS of 1.6 months and lower CD8+T cell infiltrates in prelerapolturev tumor biopsies. In peripheral blood, four patients with PFS 2.3 years (including three that received anti-PD-1 therapy within 30 days before lerapolturev and had higher pretreatment tumor CD8+T cell infiltrates) had significantly higher effector memory (CD8+, CCR7-, CD45RA-) but lower CD8+PD-1+ and CD4+PD-1+ cells compared with eight patients with median PFS 1.6 months. In addition, pretreatment blood from the four patients with median PFS 2.3 years had more potent antiviral responses to in vitro lerapolturev challenge compared with eight patients with median PFS 1.6 months.

Conclusion An inflamed pretreatment tumor microenvironment, possibly induced by prior anti-PD-1 therapy and a proficient peripheral blood pretreatment innate immune response (antiviral/interferon signaling) to lerapolturev was associated with long term PFS after intratumoral lerapolturev in a small cohort of patients.

These findings imply a link between intratumoral T cell inflammation and peripheral immune function.

Trial registration number NCT03712358.

INTRODUCTION

Both host-mediated antitumor immune responses and therapeutic strategies designed to revive antitumor host immune responses are subject to multiple tumor-driven immune suppressive mechanisms and protumorigenic signaling that occur in the tumor microenvironment (TME).¹ Cellular and molecular pathway evaluation have shown that the TME can regulate tumor progression and that altering the TME can correlate with therapeutic benefits.^{2,3} In particular, pretreatment melanoma tumors with higher intratumoral CD8⁺ T cells and increased IFN- γ signaling within the TME, so-called ‘hot tumors’, have been associated with response to anti-programmed cell death protein 1 (PD-1) therapy.^{3–5} Anti-PD-1 therapy reinvigorates intratumoral inflammation by expanding stem-like effector T cell populations in the TME, thereby altering the composition within the TME.^{6–8} Alternately, ‘cold’ tumors are characterized by minimal or absent T cell infiltration, and are less responsive to anti-PD-1 therapy.^{2,9} Among ‘cold’ tumors, phenotypes can include a lack of any appreciable T cell infiltrate or the peritumoral accumulation of T cells which are unable to enter the tumor, likely as a result of immunosuppressive myeloid cells or stroma in the TME.¹⁰ In melanoma, anti-PD-1 therapies have become the cornerstone of treatment for patients with metastatic disease and yet the majority of patients fail to respond; treatment failure

is thought to be related in part to a ‘cold’ tumor phenotype and failure to remodel the TME.¹¹ One approach for melanoma patients lacking responses to anti-PD-1 therapy is intratumoral delivery of agents designed to promote inflammation in the TME, which could potentiate responses to anti-PD-1 therapy.^{12,13}

Lerapolturev (formerly known as PVSRIPO) is the live attenuated, type 1 poliovirus (Sabin) vaccine modified with the internal ribosomal entry site of human rhinovirus type 2.¹⁴ In preclinical models, the antitumor effects of lerapolturev included tumor cell lysis and activation of antigen presenting cells in the TME, which can potentially promote a ‘hot’ tumor phenotype.^{15–17} Indeed, lerapolturev treatment of ex vivo patient tumor slice cultures culminated in robust induction of PD-L1 expression on myeloid cells; intratumor therapy of murine melanoma tumors resulted in increased tumor infiltration of PD-1-expressing CD4 and CD8 T cells and elicited functional antitumor CD8 T cell responses.^{16,17} These studies indicated potential for lerapolturev to sensitize melanoma tumors to anti-PD-1 therapy. Recently, we reported results of a phase 1 trial of intratumoral PVSRIPO in 12 patients with unresectable melanoma.¹⁸ In the phase 1 trial, four patients achieved an objective response while eight patients had no response; the injections were well tolerated. To determine immunologic effects in the TME and in the periphery, we performed tumor biopsies and blood analysis before and after lerapolturev. Here, we describe evaluation of the TME and peripheral blood analysis from melanoma patients receiving lerapolturev including the relationship of the pretreatment TME with clinical outcome, differences in pretreatment versus post-treatment tumor, comparison of results among the independent techniques used to study the tumor, and the relationship between innate activation potential in the peripheral blood and clinical outcome.

METHODS

All work was performed using Institutional Review Board approved protocols and patients signed written consent to participate. Trial details were published previously.¹⁸ Three patients received 1 injection of lerapolturev (patients 1–3), 3 patients received 2 total injections, each injection into a separate tumor (patients 4–6), 3 patients received 3 total injections each injection into a separate tumor (patients 7–9), and 3 patients received 3 total injections into the same tumor (patients 10–12).¹⁸ Tumor and peripheral blood were collected at multiple time points before and after lerapolturev. Pretreatment biopsies were collected 7–10 days prior to lerapolturev and post-treatment biopsies were performed 10 days after lerapolturev (for patients 1–9) and at median 30 days after last lerapolturev injection (for patients 11 and 12). In some cases, non-lerapolturev treated tumor was also biopsied. Flow cytometry analysis of tumor was conducted in real-time, shortly after sample collection with minimal processing to prevent exclusion or death

of innate immune cells (eg, neutrophils, basophils, and eosinophils). A separate portion of each tumor was also preserved in paraffin. For each tumor specimen, a pathologist confirmed presence of viable tumor on H&E stains; if no viable tumor was noted, the sample was not used for analysis. Flow cytometry and in vitro stimulation assays were performed using banked frozen peripheral blood mononuclear cells (PBMCs) after isolation from blood.

Flow cytometry

Tumor tissue was collected and stored in MACS tissue storage solution at 4°C (Miltenyi). Storage time was 2–16 hours post-tumor collection. Tumor cells and tumor infiltrating immune cells were analyzed after tumors were processed using the Tumor Dissociation Kit and Gentle MACS mechanical dissociator (Miltenyi) following the manufacturer’s recommendations. The suspensions were then filtered three times through a 70 µm filter to remove undigested tissue and debris. Single cell suspensions were immediately incubated with the DuraClone IM Basic panel, which contains CD16-FITC, CD56-PE, CD19-ECD, CD14-PC7, CD4-APC, CD8-AF700, CD3-AF750, and CD45-KO (Krome Orange) as previously described, to identify immune cells in tissue.¹⁹ In addition, propidium iodide (Sigma-Aldrich, St. Louis, MO) was added as a live-dead marker to single cell suspensions. Cells were incubated for 15–20 min in the dark and then washed twice in phosphate-buffered saline (PBS) prior to data acquisition. Samples were analyzed on a 13-color CytoFlex flow cytometer (Beckman Coulter). Data were analyzed using Kaluza Software (Beckman Coulter). Comparisons were made between two groups (responders and non-responders) using unpaired t-tests.

For analyses of PBMCs, frozen PBMCs were thawed in AIM-V media (Gibco) containing DNase I (1 µg/mL; Roche) and incubated for 30 min at 37°C. Cells were pelleted and resuspended in PBS (Gibco) containing Zombie-NIR stain (1:500; BioLegend) for 30 min. The cells were washed in PBS containing 2% fetal bovine serum (FBS) (Sigma-Aldrich), and resuspended in PBS+2% FBS containing human Fc block (1:100, BioLegend). The following antibodies were added for staining at a 1:100 dilution: CD3-BUV737, CD8-BUV395 (from BD Biosciences); or CD4-BV510, CD25-PERCPcy5.5, CD27-BV421, CD40L-PECF594, CD62L-FITC, PD1-BV711, CD127-PEcy5, CD45RA-APC, CD45RO-BV786, CD28-PEcy7, CD56-BV605, and CCR7-PE (all BioLegend). After 1 hour cells were washed in PBS+2% FBS and analyzed on a Fortessa X20 alongside fluorescence minus one controls for CD28, CD27, and PD1. Gating and analyses were performed using FlowJo V.10 (BD Biosciences).

In vitro PBMC stimulation assay

For in vitro stimulation of PBMCs, laboratory grade PVSRIPO was generated in HeLa cells (American Type Culture Collection, ATCC) as previously described.²⁰ Frozen, pretreatment PBMCs were thawed in AIM-V media (Gibco), treated with DNaseI (1 µg/mL; Roche)

for 30 min, counted using a Countess II automated cell counter (Thermo-Fisher), and plated in 6 wells of a 24 well plate with PBMCs at a density of 5×10^5 cells per well in RPMI-1640 (Gibco) containing 10% FBS (Sigma-Aldrich) with no other additives or added cytokines. The following stimulants were added to separate wells: mock (vehicle); PVSRIPO (1×10^7 plaque forming units (pfu)); lipopolysaccharide (LPS) (100 ng/mL; Invivogen); Pam3CSK4 (1 μ g/mL; Invivogen); R848 (1 nM; Invivogen); or combined anti-CD3 (1 μ g/mL clone OKT3; BioLegend), anti-CD28 (1 μ g/mL clone CD28.2; BioLegend), and goat anti-mouse IgG (4 μ g/mL; Jackson ImmunoResearch). Cultures were incubated for 24 hours in a 37°C and 5% CO₂ incubator, after which supernatant was harvested. Supernatant cytokines were measured using the Human Anti-Virus Response LegendPlex panel (BioLegend) on a Fortessa X20 (BD Biosciences), and the mean fluorescence intensity for each analyte was determined using the manufacturer's LegendPlex data analysis software (BioLegend). Fold mock control values were determined for each PBMC sample for each analyte.

NanoString digital spatial profiling

Formalin-fixed, paraffin-embedded (FFPE) tissue sections were analyzed using the NanoString GeoMx digital spatial profiling (DSP), a non-destructive method for high-plex spatial profiling of proteins and protein-coding genes.^{21–24} Detailed methods have been described.^{21–24} In brief, this method uses small photocleavable oligonucleotide 'barcodes' (PC oligos) covalently attached to in situ affinity reagents (antibodies and RNA probes) to provide unlimited multiplexing capability.^{21–22} The photocleavage light is projected onto the tissue slice using two-digital micromirror devices, containing 1 million semiconductor-based micromirrors allowing complete flexibility in the pattern of light utilized for high-plex digital profiling of the tissue. These spatial light patterns can be automatically configured to profile manually selected regions or molecularly defined compartments.^{21–22} Cell subset analysis can be done on a region with as low as 30 cells expressing the marker of interest. After a pathologist confirmed the presence of tumor on FFPE H&E stains, unstained slides were fluorescently stained to visualize the morphology for regions of interest (ROIs) selection and eventual proteomic or whole transcriptome analysis (WTA).^{21–22}

Statistical analysis of NanoString DSP

The protein panel included 59 proteins including internal-spike controls which were analyzed in selected ROIs. The raw data were normalized with a panel of three housekeeping proteins and three negative controls. The final step to control for variability in area and/or cellularity relies on determining the signal to noise ratio (SNR) which is calculated as the ratio of each probe over geometric mean of negative controls (mouse IgG₁, mouse IgG_{2a} and rabbit IgG). The SNR was then used to compare protein expression between our proposed ROI.

The SNR used for comparisons for each sample represents the medians from 3 to 4 ROIs (tumor or cell type). The normalized DSP SNR data of protein expression were used to create clustered heatmaps. Each heatmap row represents a patient sample and each column corresponds to a protein, with the color and intensity of the boxes indicating relative expression. The heatmaps were created using the Broad Institute's Morpheus software.²⁵ Hierarchical clustering analysis was then performed on the heatmaps. The distance measure used was the 1—Spearman correlation coefficient.²⁶ The average linkage method was used to determine the proximity between two clusters. These parameters enabled hierarchical clustering on both the rows and columns.

Similarly, the WTA analysis including 14442 human transcripts were analyzed from ROIs, normalized and the normalization values were used to make comparisons. To account and control for technical variability, a common set of external RNA controls developed by the External RNA Controls Consortium (ERCC) was used. In addition to the raw data being ERCC normalized, the raw data were normalized with a panel of three housekeeping proteins and three negative controls. After ERCC normalization a final step to control for variability in area and/or cellularity relies on determining the SNR, which is calculated as the ratio of each probe over geometric mean of negative controls. The SNR was then used to compare expression between our proposed ROI. The NanoString WTA values were analyzed using the t-test to compare the average ROIs of two groups and using a volcano plot to represent the differential expression of transcripts; fold change was calculated as mean group 1—means group 2 divided by mean group 2. If the $p < 0.05$ and fold-change $> 2 / < -2$, the genes were considered to be differentially expressed.

RRNA sequencing

Fifty micron paraffin sections of tumor were used for RNA isolation using the RNeasy FFPE kit per manufacturer's instructions by Azenta Lifesciences (formerly Genewiz). Ribosome depletion was used to enrich for mRNA. The resultant RNA quality and quantity were determined by TapeStation and Qubit assays and used for library preparation. Libraries were sequenced on an Illumina HiSeq (150 base pair (bp) paired end reads) instrument (Azenta Lifesciences). Genome alignment was performed using STAR (V.2.7.0). Differential expression analyses were performed using DESeq2 (V.3.14) and computed immune cell densities were determined using CIBERSORT.²⁷

RESULTS

Clinical data

Relevant clinical data are summarized in [table 1](#); safety results have been previously reported.¹⁸ All 12 patients with advanced unresectable melanoma had received anti-PD-1 therapy prior to lerapolturev while 6 of the 12

Table 1 Results of ppatient tumor flow cytometry analysis

Pt no	Anti PD-1 resistance	Total no Prior therapies/ prior anti-PD-1/prior anti-CTLA-4	CD3+Pre	CD3+Post	% change CD3+	CD8+ Pre	CD8+ Post	% change CD8+	CD4+ Pre	CD4+ Post	% change CD4+	Current Status
1	Primary	1/yes/no	11225	10996	-2	3274	4419	35	2907	2414	-17	Anti-CTLA-4 plus anti-PD1, alive 3.2 years
2	Primary	3/yes/yes	799	903	+13	324	389	17	152	176	16	Died 23 months
6	Primary	3/yes/yes	725			211			199			Died 11 months
3	Inadequate	2/yes/yes	18923			5237			5647			Died 20 months
4	Secondary	>10/yes/yes	13932	9452	-32	8771	4525	-48	2304	1999	-13	Died 19 months
5	Secondary	4/yes/no	8980	31697	252	1760	7968	352	3033	10228	237	Anti-PD-1, progressed 25 months, alive 2.7 years
7	Secondary	2/yes/yes	10557	55708	428	5054	24712	389	1642	9772	495	Died 9 months
10	Secondary	1/yes/yes										Died 13 months
8	Primary*	Yes/no	86395	148957	72	52799	89906	70	12387	28254	128	Anti-PD-1, alive 2.5 years
9	Primary*	Yes/no	22376			14061			2681			Anti-PD-1 alive 2.5 years
11	Secondary	Yes/no		142502			13075			125780		Anti-PD-1 alive 2.2 years
12	Primary*	Yes/no	43591	98574	126	18382	56068	205	8299	36310	338	Alive 2 years

*These patients received anti-PD-1 within 30 days of PVR5PO, therefore, confirmation of disease progression on anti-PD-1 prior to study enrolment at 4 weeks did not occur. Patients in gray are responders to lerapolturev.

patients had received both anti-PD-1 and anti-CTLA-4 therapy. Eleven of 12 patients also received anti-PD-1 therapy after lerapolturev. Primary or secondary resistance was classified according to Society for Immunotherapy of Cancer taskforce consensus.²⁸ Briefly, primary resistance is best response of progressive disease (PD) or stable disease (SD) <6 months after ≥ 6 weeks of drug exposure while secondary resistance is best response of complete response, partial response, or SD >6 months after ≥ 6 months of drug exposure.²⁸ Both definitions also include confirmatory scans at least 4 weeks after initial scan shows disease progression. After lerapolturev treatment, patient 1 (primary resistance) received anti-PD-1 plus anti-CTLA-4 (no prior exposure to anti-CTLA-4) and continues without progression at 3.2 years. Two other patients with primary resistance died at 11 and 23 months after lerapolturev. Of patients with secondary resistance (n=5), patient 11 had objective response to lerapolturev and remains free of disease at 2.2 years, patient 5 restarted anti-PD-1 therapy after lerapolturev and had disease progression after 25 months, while patients 4, 7, and 10 died after lerapolturev. Finally, among patients (8, 9, and 12) with only prior anti-PD-1 therapy and who received anti-PD-1 therapy within 30 days before lerapolturev (n=3), median progression-free survival (PFS) and overall survival (OS) after lerapolturev is 2.3 years. Two of those patients restarted anti-PD-1 therapy (8, 9) and one received no additional treatment (12). As listed in [table 1](#), all four patients with objective response to lerapolturev (patients 8, 9, 11, and 12) have no evidence of disease and have current median PFS and OS of 2.3 years.

Flow cytometry and bulk RNA sequencing of tumors

[Table 1](#) lists the absolute number of CD3+, CD8+, CD4+ cells in tumor specimens obtained before and after lerapolturev as determined using flow cytometry. Of 17 samples included in our analysis with confirmed viable tumor on matched H&E, 200,000 events were analyzed in 12 samples whereas in 5 samples the number of cells shown in [table 1](#) was normalized to 200,000 events. In [table 1](#), the absolute number of cells is listed to account for differences in the total amount of viable tumor and tumor associated melanophages in the specimens.

[Figure 1A,B](#) shows CD4+T cells and CD8+T cell densities in tumors before and after lerapolturev. Among seven patients with matched pre- and post-treatment tumors assessed via flow cytometry, two patients responded to lerapolturev and five patients had no response to lerapolturev. In three patients (non-responders), CD8+T cells decreased whereas in four patients (two non-responders and two responders) CD8+T cells increased, as listed in [table 1](#) and shown in [figure 1A](#). The mean increase in CD8+T cells across 7 patients was 13,946 (p=0.0822, paired t test). Across seven patients with matching prelerapolturev and postlerapolturev samples, the mean increase in CD4+T cells was 8998 (p=0.0522, paired t-test). The number of CD4+T cells increased in two responders, increased in two non-responders, and

appeared to be similar among the other three patients ([figure 1B](#)).

Next, we compared the differences in CD8+ and CD4+ T cells in the tumor at baseline (7–10 days prelerapolturev) between three patients with median PFS (2.3 years) vs patients 7 with median PFS 1.6 months. In 3 patients who received anti-PD-1 within 30 days prior to lerapolturev and have current median PFS 2.3 years, the mean number of CD8+T cells in the pretreatment tumor was 28,414 (n=3) compared with a mean of 3519 in 7 patients with median PFS 1.6 months after lerapolturev (p=0.0109), shown in [figure 1C](#). Although the pretreatment tumor sample for patient 11, who has PFS 2.2 years was not evaluable, the post treatment tumor had 13,075 CD8+T cells. Similarly, the mean pretreatment number of CD4+T cells in patients with median PFS 2.3 years (n=3) was 7789 compared with 2269 (n=7) in patients with median PFS 1.6 months (p=0.0261), shown in [figure 1C](#). These results were corroborated by immune cell enrichment as determined by CIBERSORT²⁷ analysis of prelerapolturev bulk RNA sequencing data of tumors ([figure 1D](#), online supplemental figure S1). Patients 8, 9 and 12 (received anti-PD-1 within 30 days prior to lerapolturev with PFS (2.3 years)) had significantly higher enrichment of CD8+T cells (p=0.0134) and activated CD4+memoryT cells (p=0.0167), compared with seven patients with median PFS 1.6 months after lerapolturev, shown in [figure 1D](#). Patient 8 (PFS 2.5 years) had the highest number of CD8+T cells as assessed by both flow cytometry and bulk RNA sequencing with patient 9 (PFS 2.5 years) having the second highest number of CD8+T cell as assessed by both flow cytometry and RNA sequencing (online supplemental figure S1). Finally, bulk RNA sequencing revealed that patient 5 (PFS progressed at 25 months) had markedly higher levels of neutrophils in the TME compared with other patients (online supplemental figure S1).

DSP of tumors

To further examine the TME, we used NanoString DSP. Images after fluorescent staining (CD3, CD163, CD11c, DNA) and H&E stains for all prelerapolturev specimens are shown in [figure 2](#). Each image also lists the number of CD3+T cells in the TME as determined by flow cytometry. The H&E for patient 11 (PFS 2.2 years) prelerapolturev sample shows necrotic tumor, and therefore, this sample was not included in all tumor analyses. This was thought to be a sampling error because the postlerapolturev biopsy for patient 11 did have viable tumor. As shown in [figure 2](#) and similar to flow cytometry and bulk RNA sequencing results, patients 8, 9, and 12 (received anti-PD-1 within 30 days prior to lerapolturev with PFS 2.3 years) had markedly higher tumor infiltrating immune cells compared with patients 1–7 (median PFS 1.6 months).

[Figure 3](#) details patient 2 and patient 8 as examples of DSP. Patient 2 (primary resistance, OS 23 months) had minimal immune infiltrate and the few CD3 cells present were in the periphery of the tumor, consistent with an

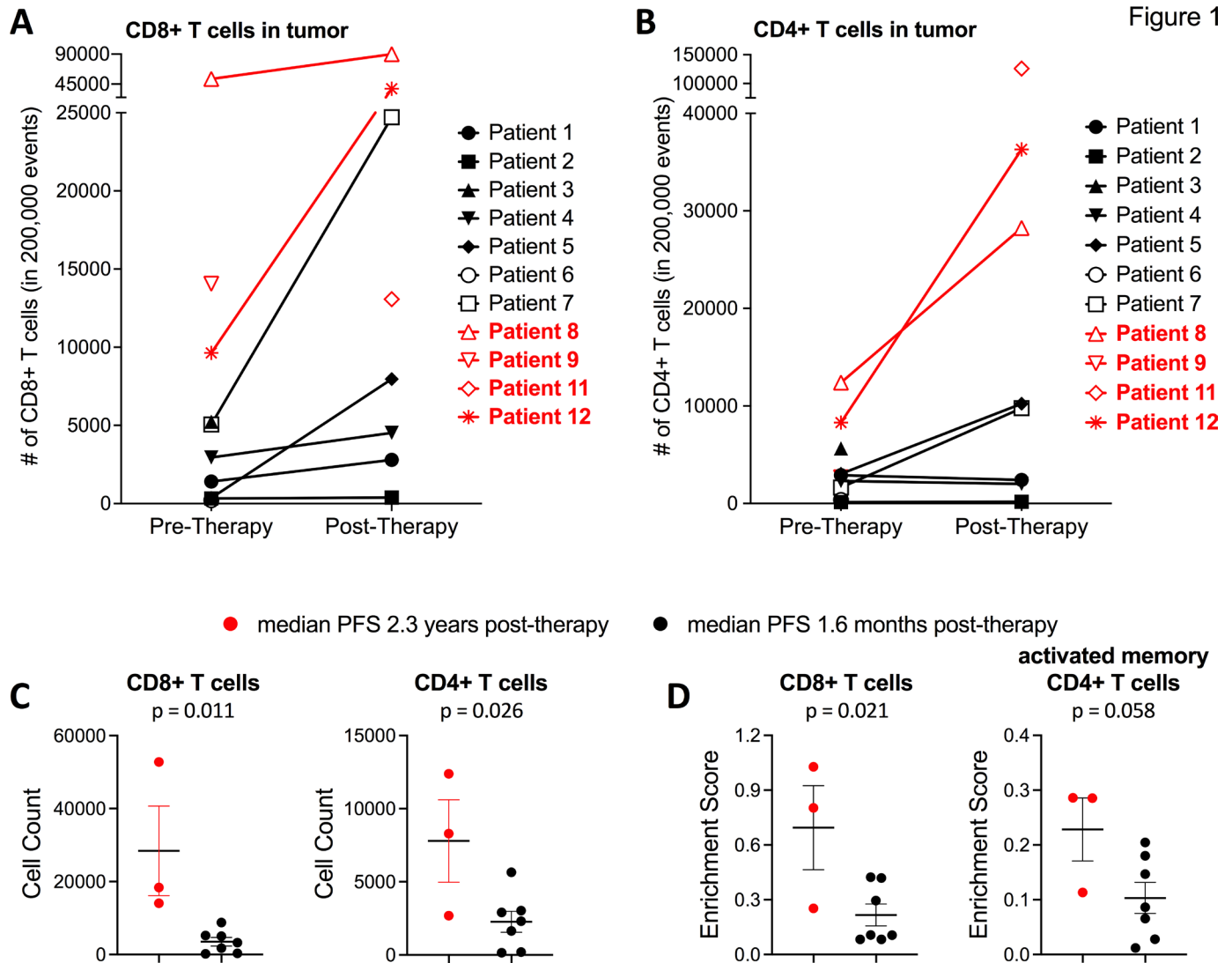


Figure 1

Figure 1 Flow cytometry and RNA sequencing analysis of tumor tissue. (A) Number of CD8+T cells and (B) number of CD4+T cells in tumor tissue as assessed by flow cytometry of fresh tumor tissue. (C)- Number of CD8+T cells (left) and CD4+T cells (right) in pretreatment tumor tissue. (D) CIBERSORT predicted (bulk RNA-sequencing) enrichment of CD8+T cells and active memory CD4+T cells in pretreatment tumor tissue. Please see online supplemental figure S1 for full heatmap of CIBERSORT enrichment scores for each patient. Patients in red have current median PFS 2.3 years compared with patients in black text with median PFS 1.6 months. PFS, progression-free survival.

immune excluded profile. There were minimal differences between the prelerapolturev and postlerapolturev samples in patient 2 as assessed by DSP and flow cytometry (figure 3). Patient 8 (prior therapy was 6 cycles of anti-PD-1 therapy, with last dose of anti-PD-1 within 30 days of lerapolturev, current OS 2.5 years) had more abundant immune cells compared with patient 2 (figure 3). There were no clear differences between the prelerapolturev and postlerapolturev biopsy in patient 8 (figure 3).

For all patients with tumor available, slides were also fluorescently stained (DNA, CD3, CD11c, and CD163) and ROIs were selected for DSP analysis as shown in figure 3; ROIs were selected based on geometric location of tumor, examples of tumor regions are shown in figure 3F. Protein values below background were excluded and geometric regions intended to represent tumor that lacked MART-1 (melanoma marker) expression below threshold were also

excluded. A heatmap of protein expression (13 proteins) in prelerapolturev tissue relevant to the melanoma TME is shown in figure 3I. The values used for the heatmap are the mean SNR from at least two ROIs for each tumor sample. Online supplemental table 1 lists all SNR values used for comparison. Interestingly, patients 8, 9, and 12 (received anti-PD-1 within 30 days of lerapolturev with median PFS 2.3 years) clustered together with higher but not significantly different mean HLA-DR expression (389.7 vs 21), higher mean CD45 expression (307.3 vs 36.4), higher mean CD8 expression (159 vs 9.6), and higher Ki-67 expression (99.6 vs 25.18) compared with prelerapolturev tumor from patients with median PFS 1.6 months (n=7) (figure 3I). This finding is also consistent with flow cytometry and bulk RNA sequencing where mean CD8+T cells from prelerapolturev tumor in patients 8, 9, and 12 (received anti-PD-1 within 30 days prior to

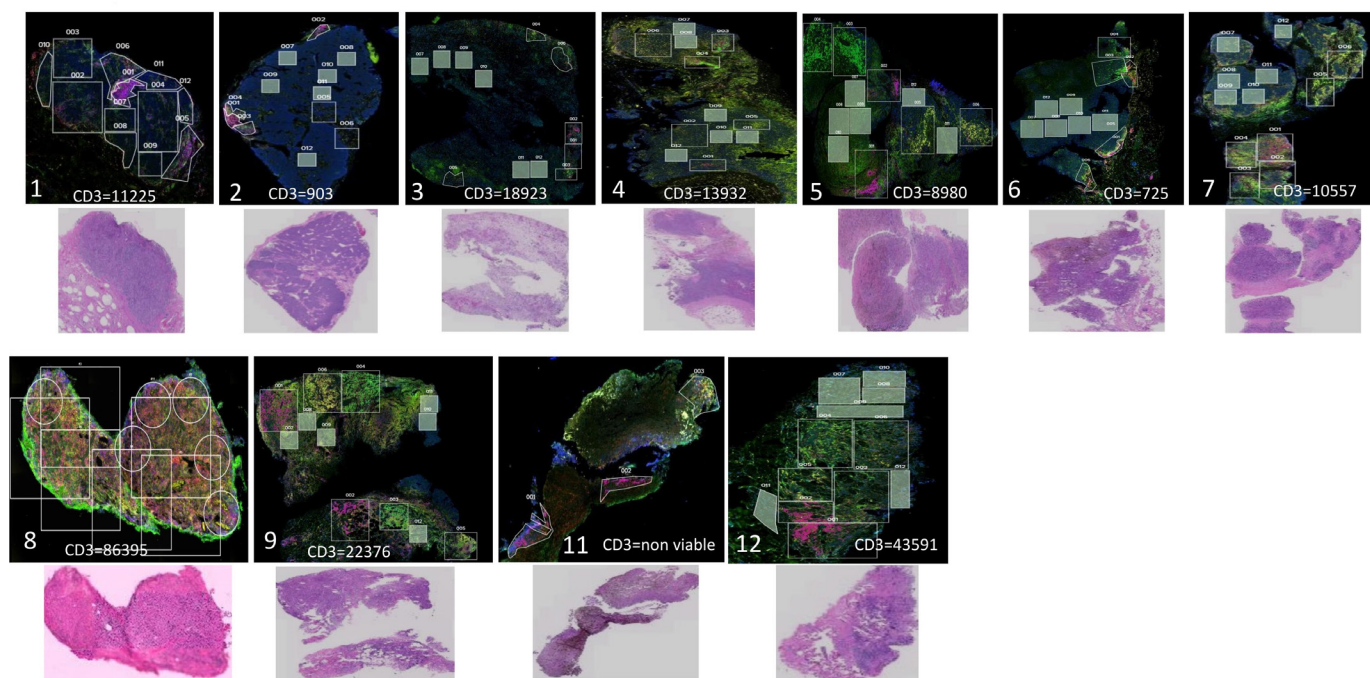


Figure 2 Analysis of tumor tissue sections. NanoString Digital Spatial Profiling (DSP) low power fluorescent images of pre-treatment tumor tissue; CD3=red, CD11c=yellow, CD163=green, DNA=blue. All images are ‘low power’= 2 mm field of view, 100x total magnification. Number in left lower corner indicates patient number. Top row, patients with median PFS 1.6 months after lerapolturev. Bottom row, patients with median PFS 2.3 years after lerapolturev. The number of CD3+T cells as assessed by flow cytometry is also shown for each tumor. Below the DSP images, a corresponding H&E stain is also shown. Note for patient 11, the H&E demonstrates near 100% necrotic tissue in the pretreatment biopsy, as such this was dropped from analysis. PFS, progression-free survival.

lerapolturev with PFS 2.3 years) were markedly higher compared with mean pretreatment CD8+T cells from pretreatment tumor in 7 patients with median PFS 1.6 months (28414 vs 3519). Among 7 patients with matched prelerapolturev and postlerapolturev tumor available for DSP, there were no consistent patterns of change from prelerapolturev to postlerapolturev tumor in expression of the 13 proteins.

The limitation to selecting geometric tumor region is that some tumors have a visual pattern of infiltrative immune cells (patient 8; [figure 3F and H](#)), precluding geometric separation of immune cells vs tumor, while visually other tumors had regions with tumor cells only or had immune cells only in scattered regions (Patient 2; [figure 3B and D](#)). A comparison of the protein expression on immune cells only may provide insight into important differences about the properties of tumor infiltrating immune cells. Accordingly, we also performed protein selection on only CD3+ cells from tumors to determine the protein expression of CD3+ cells in the TME ([figure 3](#)). Online supplemental table 1 includes SNR for all proteins. [Figure 3J](#) shows expression of 12 proteins involved in T cell signaling in prelerapolturev tumor tissue from CD3+ cells only. It should be noted that expression of some markers such as MART-1 were present on CD3 cells (online supplemental table S1), suggesting there is some background protein expression not confined to CD3+ cells. As expected, CD44 was high

all for all patients since only CD3+ cells were selected for analysis. Patient 8, 9, and 12 (received anti-PD-1 therapy within 30 days of lerapolturev with median PFS 2.3 years) grouped together based primarily on high expression of CD8 compared with other patients. Among 7 patients with matched prelerapolturev and postlerapolturev tumor available for DSP, there were no consistent patterns of change from prelerapolturev to postlerapolturev tumor in expression of the 12 proteins on CD3+T cells.

We noted that while patients 8, 9, 12 (median PFS 2.3 years) appeared to have a more inflamed tumor profile primarily driven by CD8+T cells, other patients namely 5 (PFS 25 months) and 7 (death at 7 months) also had immune cell infiltrates within the TME visualized by fluorescent staining ([figure 2](#)). To explore differences in these immune infiltrates such as the presence of T regulatory or other suppressor cells that may have led to the different clinical outcomes, we performed WTA on tumor from patients with immune infiltrates in tumor. FFPE tumor tissue sections from patients 8, 9, 12, (group 1) and patients 5 and 7 (group 2) were fluorescently stained for CD8 (teal), CD4 (red), CD11c (green), and DNA (blue, tumor) as shown in [figure 4A,B](#). ROIs were then selected for areas enriched with CD8 and CD4 cells; WTA on cells only expressing the specific marker (either CD4 or CD8) was then performed as shown in [figure 4A,B](#). At least two ROIs were selected for each cell type. Among 14442 human transcripts, we examined differences in

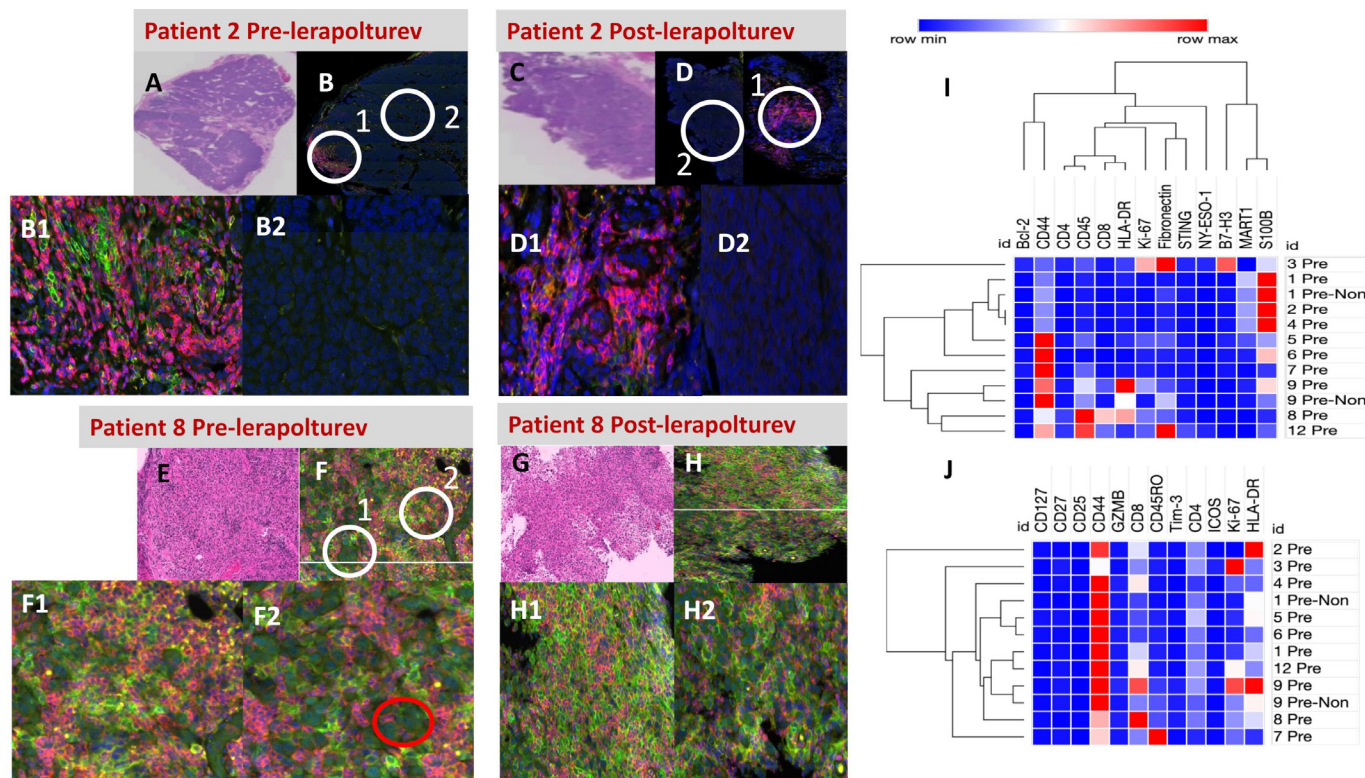


Figure 3 NanoString Digital Spatial Profiling (DSP) of tumor tissue. Top left and middle panel, ‘low power’ = 2 mm field of view, 100x total magnification, ‘high power’ = 45µm field of view, 400x total magnification. (A, B) Patient 2 prelerapolturev and (C, D) post-lerapolturev tumor. (A, C) Corresponding H&E. (B) DSP low power, fluorescent image, CD3=red, CD11c=yellow, CD163=green, DNA=blue. Same fluorescent markers also present in (D, F, H). B1—High power view of region 1 circled (white circle) in image B. (B2) High power view of region 2 circled (white circle) in image B. (D) DSP image low power, tumor cells can be identified as cells with irregular blue nucleus. D1—High power view of region 1 circled (white circle) in image D. D2—High power view of region 2 circled (white circle) in image D. Bottom left and middle (E, F) Patient 8 prelerapolturev and G, H postlerapolturev tumor. (E, G) Corresponding H&E stains. (F) DSP image low power. (F1) High power view of region 1 circled (white circle) in image F. (F2) High power view of region 2 circled (white circle) in image F. Tumor cells can be identified as cells with irregular blue nucleus depicted in F2, red circle. H- DSP image low power. (H1) High power view of region 1 circled (white circle) in image H. (H2) High power view of region 2 circled (white circle) in image (H. I, J) Heatmaps of selected protein expression obtained from tumor regions of interest in (I) pretreatment tumor tissue and (J) CD3+compartment only. Patient identification on the y axis (right), pre-NON is pretreatment tissue collected without lerapolturev injection.

CD4+cells and CD8+cells between patients 8, 9, and 12 (group 1) and patients 5 and 7 (group 2). There were no significant differences in CD4+ transcripts between the two groups. Among CD8+ transcripts, five genes were significantly differentially expressed by more than twofold as shown in [figure 4C](#), including higher HLA-DQA1, MIA (melanoma inhibitory activity), SERPINA3 (Serpin Peptidase Inhibitor, clade A member 3), KRTAP5-8 (keratin-associated protein 5–8), and XAGE1A (human cancer/testis antigens X-antigen family member 1) in group 1. These differences may reflect distinct activation status of CD8+T cells from patients 8, 9, and 12 (median PFS 2.3 years) compared with CD8+T cells from patients 5 (progressed at 25 months) and 7 (death at 7 months). Although this methodology analyzes only cells expressing the selected fluorescent marker (CD4+ or CD8+) there may also be background expression from tumor cells.

Analysis of peripheral blood

Immune subsets in blood were also analyzed at multiple time points. Patients with PFS 2.3 years after lerapolturev

(patients 8, 9, 11, 12), which includes the three patients who had received anti-PD-1 therapy within 30 days before lerapolturev (8, 9, and 12) had significantly higher numbers of CD8+CCR7+CD45RA- T effector memory cells, but significantly lower CD8+PD-1+, and CD4+PD-1+ T cells compared with 8 patients with median PFS 1.6 months after lerapolturev ([figure 5](#) and online supplemental figure S2). Patients 8, 9, and 12 (median PFS 2.3 years) had received a mean of 6 cycles of prior anti-PD-1 therapy prior to trial entry with last dose within 30 days before lerapolturev. No other correlations with response or changes prelerapolturev to postlerapolturev were noted.

In preclinical studies, PVSRIPO (lerapolturev) mediated antitumor efficacy by inducing type-I IFN dominant innate inflammation in myeloid cells via the cytoplasmic pattern recognition receptor MDA5.^{16 17} Moreover, recent evidence indicates that patient-specific differences in peripheral blood responsiveness to type I interferon associates with outcome after anti-PD-1 therapy in patients.²⁹

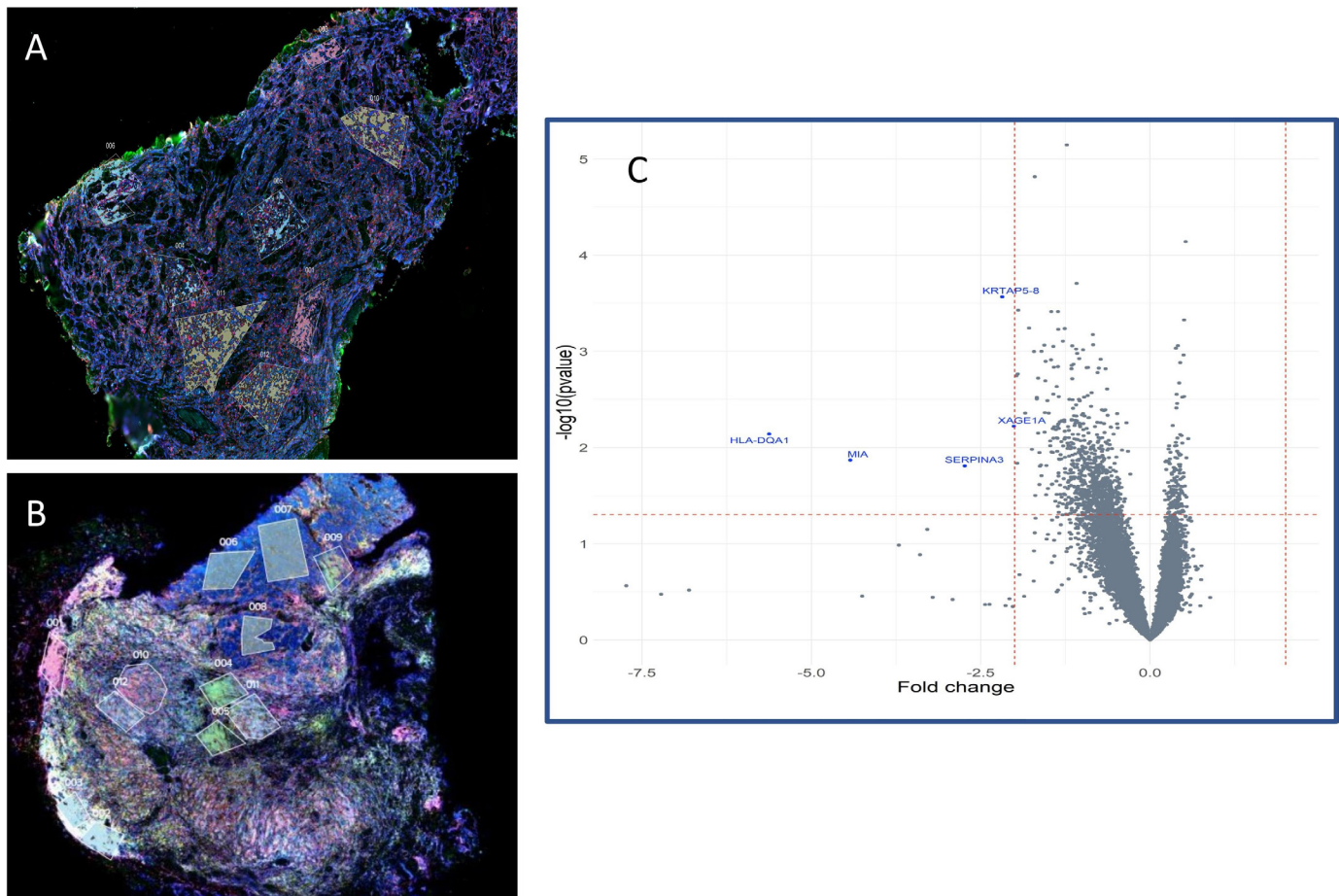


Figure 4 NanoString Digital Spatial Profiling (DSP) of tumor tissue. NanoString DSP images after fluorescent staining on pretreatment tissue, CD8=teal, CD4=red, CD11c=yellow, and DNA=blue. ‘Low power’ = 2 mm field of view, 100× total magnification. Rectangles indicate ROIs selected based on enrichment for cell type or tumor. (A) Low power image patient 12. (B) Low power image patient 7. (C) Volcano plot comparing ROI on CD8+ cells only between patients 8, 9, 12, 5 and 7. Differentially expressed genes appear in blue. ROI, regions of interest.

We previously discovered that lerapolturev infects and induces cytokine responses in monocytes, but not T/B cells in PBMCs after 24 hours of treatment.¹⁷ Thus, we next asked if peripheral capacity to induce antiviral inflammation after lerapolturev infection associates with therapy outcome, possibly by reflecting the capacity of a patient’s innate immune system to respond to lerapolturev treatment or by reflecting the status of peripheral innate immunity at the time of treatment. To this end, we developed a peripheral immune function assay that measured pro-inflammatory cytokine responses of pretreatment PBMCs after in vitro challenge with lerapolturev or other innate stimuli to broadly probe innate immune status, including the TLR4 agonist LPS, the TLR1/2 agonist Pam3CSK4, and the TLR7/8 agonist R848 (figure 6; online supplemental figures S3 and S4). Since we observed higher levels of effector memory T cells in peripheral blood (figure 5) and tumor infiltrating T cells (figure 1) in patients living longer after lerapolturev therapy, we also compared responses to T cell stimulation using CD3/CD28 ligation. The fold increase in cytokine production after 24 hours of stimulation with lerapolturev over mock treatment is shown (figure 6; online supplemental figures S3 and

S4). Patients with median PFS 2.3 years after lerapolturev (patients 8, 9, 11, 12) including the 3 patients with known prelerapolturev inflamed TME who received anti-PD-1 therapy within 30 days before lerapolturev (patients 8, 9 and 12), had significantly higher production of IFN- β , IFN- λ 2, IFN- γ , and GM-CSF compared with eight patients with median PFS 1.6 months after lerapolturev. In addition, CXCL10 production was higher after LPS and anti-CD3/28 treatment in the four patients with PFS 2.3 years after lerapolturev compared with eight patients with median PFS 1.6 months (online supplemental figures S3). No difference in baseline cytokine secretion (Mock treatment) was observed between patients with PFS 2.3 years vs PFS 1.6 months, indicating the aforementioned superior poststimulation cytokine levels in patients with PFS 2.3 years were due to differential sensitivity to in vitro stimulation (online supplemental figures S4). Together, peripheral prelerapolturev immune responsiveness (figure 6) with the increased T cell inflammation in prelerapolturev tumors and higher levels of effector memory CD8+T cells in prelerapolturev periphery of patients with PFS 2.3 years, imply that an active and/or proficient

Figure 5

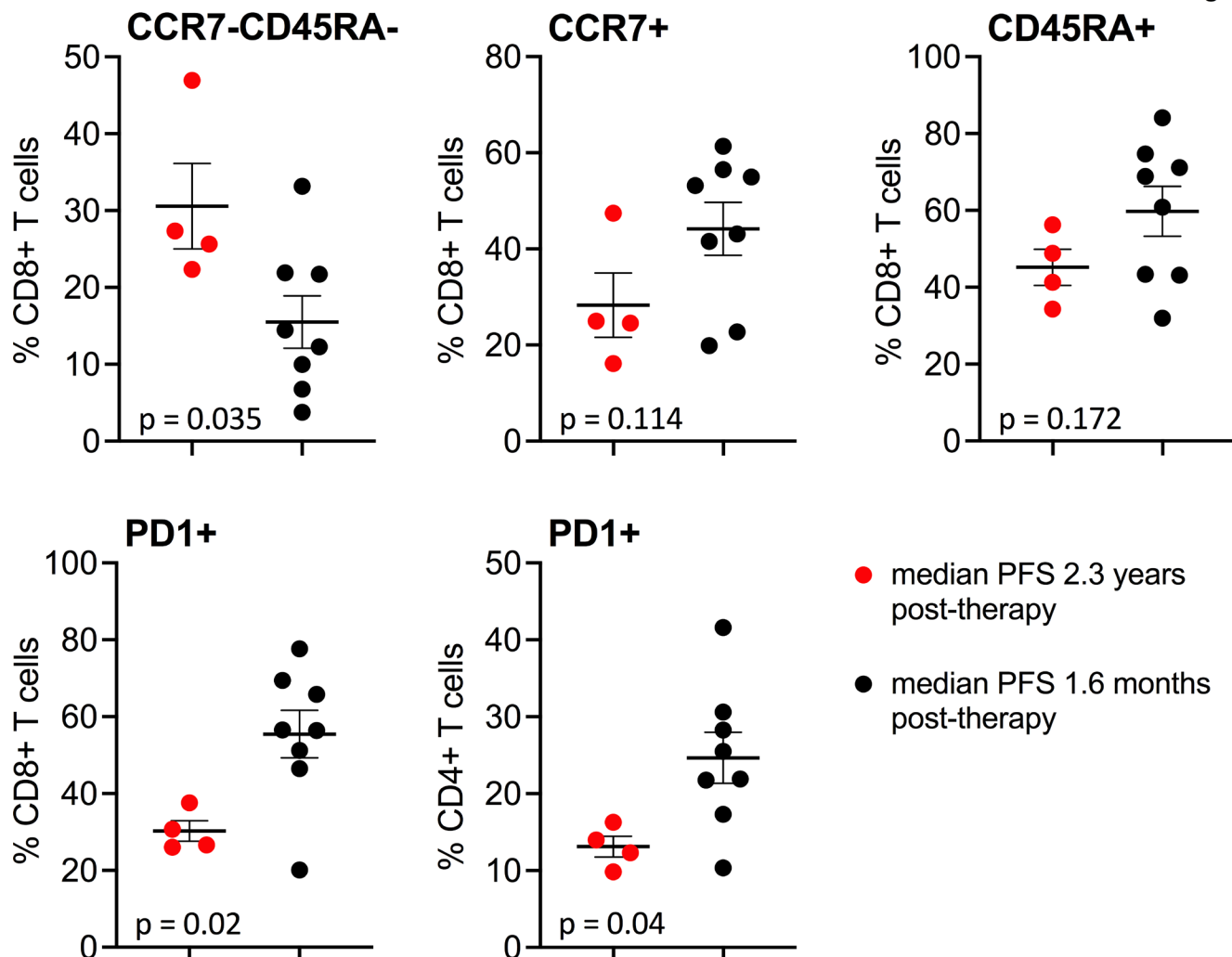


Figure 5 Flow cytometry analysis of immune subsets in peripheral blood. PBMCs were analyzed for T cell memory populations and PD1 expression on CD8+ and CD4+ conventional T cells as shown at the pretreatment time point. Patients in red have median PFS of 2.3 years after lerapolturev and patients in black have median PFS 1.6 months after lerapolturev. Data brackets indicate mean \pm SEM; p values are from unpaired t-test. PBMCs, peripheral blood mononuclear cells; PFS, progression-free survival.

immune status at baseline in patients may result in favorable clinical outcomes.

DISCUSSION

The presence of tumor infiltrating lymphocytes (TILs) and an inflamed tumor in precheckpoint inhibitor therapy tumor (baseline) is associated with improved OS in melanoma and predictive of response to ICI therapy.^{30–32} Using three separate modalities—flow cytometry, DSP (protein and WTA), and RNA sequencing—we observed that three patients with advanced melanoma and a median PFS of 2.3 years had markedly elevated TILs in prelerapolturev tumor compared with seven patients with less abundant TILs in pretreatment tumors and median PFS 1.6 months. Although this observation aligns with previous findings that responses to immunotherapy preferentially occur in tumors with an ‘inflamed’

phenotype, our study is limited by a small sample size.³¹ Furthermore, in matching prelerapolturev blood (baseline) from the same three patients with an inflamed TME, median PFS 2.3 years and a fourth patient with PFS 2.2 years (no prelerapolturev tumor available in the fourth patient), a more pronounced peripheral innate immune response to in vitro lerapolturev challenge was observed compared with eight patients with median PFS 1.6 months (including seven patients with non-inflamed prelerapolturev tumor). Findings in peripheral blood are also limited by small sample size. Among the eight patients with PFS 1.6 months, six patients have died while current PFS and OS among the other four patients is 2.3 years.

Determining clinical and radiographic responses to anti-PD-1 therapy can be complicated by delayed responses and pseudoprogression.²⁸ Guidelines that more precisely define anti-PD-1 failure predated our

Figure 6

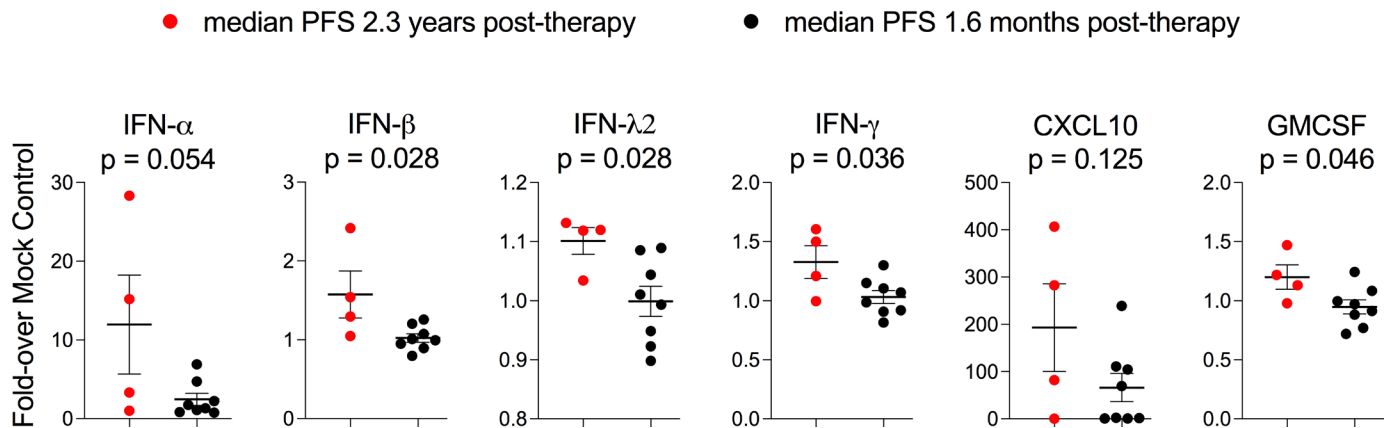


Figure 6 Assessment of baseline peripheral immune cell function in response to lerapolturev. PBMCs from the pretreatment time point were challenged with laboratory grade PVSR1PO in vitro for 24 hours. Supernatant was tested for proinflammatory cytokines. Patients in red have median PFS of 2.3 years after lerapolturev and patients in black have median PFS 1.6 months after lerapolturev. Data brackets indicate mean \pm SEM; p values are from unpaired t-test. See online supplemental figure S3 for complete results of cytokines and stimuli tested; online supplemental figure S4 presents baseline raw MFI and concentration of cytokines for all stimuli. GMCSF, granulocyte-macrophage colony-stimulating factor; MFI, mean fluorescence intensity; PBMCs, peripheral blood mononuclear cells; PFS, progression-free survival.

study design and as such five patients received anti-PD-1 therapy within 30 days of lerapolturev, although clinically these patients appeared to be progressing. Three of those patients (8, 9, and 12) had the highest number of CD8+T cells (mean 28,414) in prelerapolturev tumor (tumor biopsied within 30 days of anti-PD-1 therapy prelerapolturev) compared with mean value of 3509 (n=7) in other patients. This was consistent with bulk RNA sequencing and DSP analysis. In addition, patient 11 with PFS 2.2 years, had a higher number (13 075 CD8+T cells) in postlerapolturev tumor. Together, those four patients (8, 9, 11, 12) continue to have prolonged PFS (median 2.3 years vs 1.6 months median PFS for the other seven patients). Interestingly, patient 9's (PFS 2.5 years) prelerapolturev non-treated lesion also had marked tumor inflammation while patient 1's (SD after initiation of anti-CTLA-4 plus anti-PD-1) prelerapolturev non-treated lesion had little immune infiltrate (figure 3J). Therefore, it is possible that anti-PD-1 therapy contributed to disease control for patient 8, 9, and 12, (median PFS 2.3 years) since the last dose of anti-PD-1 therapy was within 30 days and the TME of those patients had a more inflamed tumor profile prior to lerapolturev. However, lerapolturev may have provided additional support of inflammation and remodeling of the TME. Recent data suggest that there are T cell infiltrated tumors that are resistant to anti-PD-1 possibly due to lack of coexisting proinflammatory cytokines.³³ Oncolytic viruses like lerapolturev may provide this type of inflammation which can lead to a clinical benefit as we observed in four patients on the study.

Use of spatial biology in our study in addition to flow cytometry and bulk RNA sequencing highlighted interesting aspects about studying the TME. Intratumoral heterogeneity was observed which is most apparent when viewing DSP images, which preserves spatial biology. Some

patients had portions of tumor with abundant TILs, some had TILs only on the tumor periphery, and some patients had TILs arranged in an infiltrative pattern. Those relationships are not as easily captured using flow cytometry or bulk RNA sequencing.³⁴ However, flow cytometry can provide more detailed information about live cells, and bulk RNA sequencing evaluates a larger spectrum of cell types. Although CD8+T cell infiltrated tumors are a known predictor of response to anti-PD-1 therapy, about 30% of patients with CD8+T cells in the tumor will still not respond to checkpoint therapy.³³ WTA of CD8+T cells among two groups of patients, both with CD8+T cells present in tumor but with divergent outcomes revealed differences in the CD8+T cells that may in part explain the divergence. The higher HLA-DQA1 on CD8+T cells from patients with prolonged PFS suggests robust T cell activation.³⁵ Spi2A, is encoded by SERPINA3. Spi2A enhances the initial development of memory CD8+T cells and SERPINA3 was markedly increased on CD8+T cells from patients with prolonged PFS.³⁶

Given the intratumoral heterogeneity and limitations of biopsies which do not evaluate the entire tumor, we also conducted blood analysis. Identification of a blood-based biomarker could also be a useful approach to evaluate therapy efficacy in larger clinical studies given that blood is easier to obtain, non-invasive, and facilitates longitudinal analysis of changes in the immune system. Previous reports indicate that anti-PD-1 therapy induces proliferation of CD8+PD-1+ and CD4+PD-1+ T cells in peripheral blood with the increase peaking at 1 week after initiating anti-PD-1 and then decreasing thereafter despite continuous anti-PD-1 treatment.^{37 38} Therefore, the finding that three of four patients with prolonged PFS (2.3 years) in our study had lower CD8+PD-1+ and CD4+PD-1+ T cells is not surprising since three of four patients with prolonged

PFS had received an average of six cycles of anti-PD-1 with last dose within 30 days prior to lerapolturev while only two of eight patients with poor PFS had received anti-PD-1 within 30 days.

Since anti-PD-1 therapy works by expanding functional effector T cells in the TME and lerapolturev also recruits peripheral blood innate immune cells in the TME, we investigated if immune function in blood could predict presence of immune cells in the TME or ability to recruit peripheral cells into the tumor.^{6,7} Three patients who received anti-PD-1 within 30 days of lerapolturev, who had an inflamed prelerapolturev TME as noted by flow cytometry, DSP, and RNA sequencing, and had PFS 2.3 years, appeared to elicit a robust response in peripheral blood as measured by cytokine production after in vitro stimulation with lerapolturev (and in some cases LPS and anti-CD3/CD28 stimulation) compared with eight patients with median PFS 1.6 months. A fourth patient (11) with no prelerapolturev tumor available (but who had an inflamed post lerapolturev TME), with PFS 2.2 years also mounted a robust response in peripheral blood after in vitro stimulation with lerapolturev. Of note, all four patients with prolonged PFS (2.3 years) and robust innate immune response had only received anti-PD-1 therapy prior to lerapolturev while all other patients were more heavily pretreated (table 1). This type of analysis may be useful in assessing peripheral innate immune responsiveness/competence and may predict which therapies can effectively recruit immune cells into the TME for an individual patient. Four patients with the most robust cytokine response had the highest levels of T cells in the TME.

A current trial, LUMINOS-102 (lerapolturev with or without immune checkpoint blockade) in patients with advanced PD-1 refractory melanoma (NCT04577807) is ongoing. Patients will have confirmed progression on anti-PD-1 therapy before enrollment. In treatment naïve patients, final results of MASTER-KEY-265 suggested that the intratumoral oncolytic virus, talimogene laherparepvec plus pembrolizumab did not significantly improve PFS or OS compared with placebo plus pembrolizumab in a large phase III randomized study.³⁹ Therefore, intratumoral therapies may be more relevant for selected patients not initially responding to checkpoint therapy as is being explored in LUMINOS-102. In addition, the mechanisms of lerapolturev are unique and efficacy may be different.

In conclusion, patients with a prelerapolturev inflamed TME and increased sensitivity to in vitro lerapolturev challenge in prelerapolturev peripheral blood had prolonged median PFS (2.3 years) after treatment with lerapolturev compared with patients with median PFS of 1.6 months, who had prelerapolturev ‘cold’ tumors and lower cytokine response in prelerapolturev peripheral blood. All four patients with prolonged PFS had also received anti-PD-1 therapy (three of 4 within 30 days of lerapolturev) and no additional systemic therapies. Given this observation in our pilot study in 12 patients,

future studies will test if immune response measured in the periphery (blood) may be important in predicting ability to recruit immune cells into the TME in a larger cohort of patients.

Author affiliations

¹Department of Surgery, Duke University, Durham, North Carolina, USA

²Department of Medicine, Duke University, Durham, North Carolina, USA

³Department of Neurosurgery, Duke University, Durham, North Carolina, USA

⁴Department of Pathology, Duke University, Durham, North Carolina, USA

⁵Department of Biostatistics and Bioinformatics, Duke University, Durham, North Carolina, USA

⁶Department of Molecular Genetics and Microbiology, Duke University, Durham, North Carolina, USA

Contributors GMB, MCB, NF, KL, RA, AS, AT, SHJ, JG, DB, EH, AKS, DDB, MG and SKN, made substantial contributions to the conception and design of the work. GMB, MCB, NF, KL, RA, AS, AT, SHJ, JG, DB, EH, AKS, DDB, MG and SKN made significant contributions to data acquisition, analysis, and interpretation of data for the work. GMB, MCB and SKN made significant contributions to drafting the manuscript and critical revision for important intellectual content. All authors gave the final approval of the version to be published. All authors were accountable to ensure that questions related to the accuracy or integrity of any part of the work were appropriately investigated and resolved. GMB, MCB, and SKN are responsible for the overall content as guarantors. GMB, MCB, and SKN accept full responsibility for the finished work and/or the conduct of the study, had access to the data, and controlled the decision to publish.

Funding NIH K08 CA237726-01A1 and the Duke Cancer Institute's Pilot Grant (P30 Cancer Center Grant NIH CA014236) to GMB; NIH K99CA263021 to MCB, NIH T32 grant (T32-CA093245) for translational research in surgical oncology to NEF and KL, and DoD Breast Cancer Research Program award W81XWH-16-1-0354 to SKN.

Competing interests GMB reports clinical trial funding from Istari Oncology, Delcath, Oncosec Medical, Replimune, and Checkmate Pharmaceuticals paid to Duke University. AnS receives research funding paid to the institution from Bristol Myers Squibb, Immunocore, Merck, Pfizer Advisory roles; and has served on advisory boards for Array, Novartis, Iovance, and Regeneron. MCB, DDB and MG are paid consultants of Istari Oncology, Inc. and MG and DDB are scientific advisors for Istari Oncology; DDB and MG hold equity in Istari Oncology. MCB, DDB, MG and SKN own intellectual property related to this research, which has been licensed to Istari Oncology. Duke University (Licensor of PVSRIP0) has a financial interest in Istari Oncology. All other authors declare they have no competing interests.

Patient consent for publication Consent obtained directly from patient(s)

Ethics approval This study involves human participants and was approved by Duke Cancer Center (no ID) Duke IRB Pro00090774 Western IRB1 IBCL-17-0046-01. Participants gave informed consent to participate in the study before taking part.

Provenance and peer review Not commissioned; externally peer reviewed.

Data availability statement All data relevant to the study are included in the article or uploaded as online supplemental information.

Supplemental material This content has been supplied by the author(s). It has not been vetted by BMJ Publishing Group Limited (BMJ) and may not have been peer-reviewed. Any opinions or recommendations discussed are solely those of the author(s) and are not endorsed by BMJ. BMJ disclaims all liability and responsibility arising from any reliance placed on the content. Where the content includes any translated material, BMJ does not warrant the accuracy and reliability of the translations (including but not limited to local regulations, clinical guidelines, terminology, drug names and drug dosages), and is not responsible for any error and/or omissions arising from translation and adaptation or otherwise.

Open access This is an open access article distributed in accordance with the Creative Commons Attribution Non Commercial (CC BY-NC 4.0) license, which permits others to distribute, remix, adapt, build upon this work non-commercially, and license their derivative works on different terms, provided the original work is properly cited, appropriate credit is given, any changes made indicated, and the use is non-commercial. See <http://creativecommons.org/licenses/by-nc/4.0/>.

ORCID iD

Georgia M Beasley <http://orcid.org/0000-0001-6387-9030>

REFERENCES

- 1 Jacquelinot N, Roberti MP, Enot DP, *et al.* Predictors of responses to immune checkpoint blockade in advanced melanoma. *Nat Commun* 2017;8:592.
- 2 Erdag G, Schaefer JT, Smolkin ME, *et al.* Immunotype and immunohistologic characteristics of tumor-infiltrating immune cells are associated with clinical outcome in metastatic melanoma. *Cancer Res* 2012;72:1070–80.
- 3 Horton BL, Williams JB, Cabanov A, *et al.* Intratumoral CD8+ T-cell apoptosis is a major component of T-cell dysfunction and impedes antitumor immunity. *Cancer Immunol Res* 2018;6:14–24.
- 4 Sharma P, Hu-Lieskovan S, Wargo JA, *et al.* Primary, adaptive, and acquired resistance to cancer immunotherapy. *Cell* 2017;168:707–23.
- 5 Wei SC, Levine JH, Cogdill AP, *et al.* Distinct cellular mechanisms underlie anti-CTLA-4 and anti-PD-1 checkpoint blockade. *Cell* 2017;170:1120–33.
- 6 Hegde PS, Karanikas V, Evers S. The where, the when, and the how of immune monitoring for cancer immunotherapies in the era of checkpoint inhibition. *Clin Cancer Res* 2016;22:1865–74.
- 7 Taube JM, Klein A, Brahmer JR, *et al.* Association of PD-1, PD-1 ligands, and other features of the tumor immune microenvironment with response to anti-PD-1 therapy. *Clin Cancer Res* 2014;20:5064–74.
- 8 Siddiqui I, Schaeuble K, Chennupati V, *et al.* Intratumoral Tcf1+PD-1+CD8+ T cells with stem-like properties promote tumor control in response to vaccination and checkpoint blockade immunotherapy. *Immunity* 2019;50:195–211.
- 9 Sharma P, Allison JP. The future of immune checkpoint therapy. *Science* 2015;348:56–61.
- 10 Herbst RS, Soria J-C, Kowanetz M, *et al.* Predictive correlates of response to the anti-PD-L1 antibody MPDL3280A in cancer patients. *Nature* 2014;515:563–7.
- 11 Robert C, Long GV, Brady B, *et al.* Five-Year Outcomes With Nivolumab in Patients With Wild-Type BRAF Advanced Melanoma. *J Clin Oncol* 2020;38:3937–46.
- 12 Ribas A, Dummer R, Puzanov I, *et al.* Oncolytic virotherapy promotes intratumoral T cell infiltration and improves anti-PD-1 immunotherapy. *Cell* 2017;170:1109–19.
- 13 Cerullo V, Diaconu I, Romano V, *et al.* An oncolytic adenovirus enhanced for toll-like receptor 9 stimulation increases antitumor immune responses and tumor clearance. *Molecular Therapy* 2012;20:2076–86.
- 14 Gromeier M, Lachmann S, Rosenfeld MR, *et al.* Intergeneric poliovirus recombinants for the treatment of malignant glioma. *Proc Natl Acad Sci U S A* 2000;97:6803–8.
- 15 Holl EK, Brown MC, Boczkowski D, *et al.* Recombinant oncolytic poliovirus, PVSRIPO, has potent cytotoxic and innate inflammatory effects, mediating therapy in human breast and prostate cancer xenograft models. *Oncotarget* 2016;7:79828–41.
- 16 Brown MC, Holl EK, Boczkowski D, *et al.* Cancer immunotherapy with recombinant poliovirus induces IFN-dominant activation of dendritic cells and tumor antigen-specific CTLs. *Sci Transl Med* 2017;9.
- 17 Brown MC, Mosaheb MM, Mohme M, *et al.* Viral infection of cells within the tumor microenvironment mediates antitumor immunotherapy via selective TBK1-IRF3 signaling. *Nat Commun* 2021;12:1858.
- 18 Beasley GM, Nair SK, Farrow NE, *et al.* Phase I trial of intratumoral PVSRIPO in patients with unresectable, treatment-refractory melanoma. *J Immunother Cancer* 2021;9:e002203.
- 19 Holl EK, Frazier VN, Landa K, *et al.* Examining peripheral and tumor cellular Immunome in patients with cancer. *Front Immunol* 2019;10:10.
- 20 Brown MC, Bryant JD, Dobrikova EY, *et al.* Induction of viral, 7-methyl-guanosine cap-independent translation and oncolysis by mitogen-activated protein kinase-interacting kinase-mediated effects on the serine/arginine-rich protein kinase. *J Virol* 2014;88:13135–48.
- 21 Beechem JM. High-Plex spatially resolved RNA and protein detection using digital spatial profiling: a technology designed for Immuno-oncology biomarker discovery and translational research. *Methods Mol Biol* 2020;2055:563–83.
- 22 Toki MI, Merritt CR, Wong PF, *et al.* High-plex predictive marker detection for melanoma Immunotherapy-Treated patients using digital spatial profiling. *Clin Cancer Res* 2019;25:5503–12.
- 23 Delorey TM, Ziegler CGK, Heimberg G, *et al.* COVID-19 tissue atlases reveal SARS-CoV-2 pathology and cellular targets. *Nature* 2021;595:107–13.
- 24 Delorey TM, Ziegler CGK, Heimberg G, *et al.* A single-cell and spatial atlas of autopsy tissues reveals pathology and cellular targets of SARS-CoV-2. *bioRxiv* 2021. doi:10.1101/2021.02.25.430130. [Epub ahead of print: 25 Feb 2021].
- 25 Morpheus. Available: <https://software.broadinstitute.org/morpheus>
- 26 Spearman C. The proof and measurement of association between two things. *Am J Psychol* 1987;100:441–71.
- 27 Newman AM, Steen CB, Liu CL, *et al.* Determining cell type abundance and expression from bulk tissues with digital cytometry. *Nat Biotechnol* 2019;37:773–82.
- 28 Kluger HM, Tawbi HA, Ascierto ML, *et al.* Defining tumor resistance to PD-1 pathway blockade: recommendations from the first meeting of the SITC immunotherapy resistance Taskforce. *J Immunother Cancer* 2020;8:e000398.
- 29 Boukhalel GM, Gadalla R, Elsaesser HJ, *et al.* Pre-encoded responsiveness to type I interferon in the peripheral immune system defines outcome of PD1 blockade therapy. *Nat Immunol* 2022;23:1273–83.
- 30 Yost KE, Satpathy AT, Wells DK, *et al.* Clonal replacement of tumor-specific T cells following PD-1 blockade. *Nat Med* 2019;25:1251–9.
- 31 Gajewski TF, Corrales L, Williams J, *et al.* Cancer immunotherapy targets based on understanding the T Cell-Inflamed versus non-T Cell-Inflamed tumor microenvironment. *Adv Exp Med Biol* 2017;1036:19–31.
- 32 Fu Q, Chen N, Ge C, *et al.* Prognostic value of tumor-infiltrating lymphocytes in melanoma: a systematic review and meta-analysis. *Oncimmunology* 2019;8:1593806.
- 33 Voabil P, de Bruijn M, Roelofs LM, *et al.* An ex vivo tumor fragment platform to dissect response to PD-1 blockade in cancer. *Nat Med* 2021;27:1250–61.
- 34 Dagogo-Jack I, Shaw AT. Tumour heterogeneity and resistance to cancer therapies. *Nat Rev Clin Oncol* 2018;15:81–94.
- 35 Holling TM, Schooten E, van Den Elsen PJ. Function and regulation of MHC class II molecules in T-lymphocytes: of mice and men. *Hum Immunol* 2004;65:282–90.
- 36 Liu N, Phillips T, Zhang M, *et al.* Serine protease inhibitor 2A is a protective factor for memory T cell development. *Nat Immunol* 2004;5:919–26.
- 37 Kim KH, Cho J, Ku BM, *et al.* The First-Week Proliferative Response of Peripheral Blood PD-1⁺CD8⁺ T Cells Predicts the Response to Anti-PD-1 Therapy in Solid Tumors. *Clin Cancer Res* 2019;25:2144–54.
- 38 Huang AC, Orlowski RJ, Xu X, *et al.* A single dose of neoadjuvant PD-1 blockade predicts clinical outcomes in resectable melanoma. *Nat Med* 2019;25:454–61.
- 39 Gogas H, Ribas A, Chesney J. MASTERKEY-265: A phase 3, randomized, placebo (PBO)-controlled study of talimogene laherparepvec (T) plus pembrolizumab (P) for unresectable stage IIIB-IVM1C melanoma (MEL) 2021.